Available online at www.sciencedirect.com
ScienceDirect
Earth and Planetary Science Letters 263 (2007) 388–403
EPSL
www.elsevier.com/locate/epsl

TiO_2 enrichment in ocean island basalts

J. Prytulak *, T. Elliott [1]

Bristol Isotope Group, Department of Earth Sciences, University of Bristol, Queen's Road, BS8 1RJ, Bristol, UK

Received 5 April 2007; received in revised form 15 September 2007; accepted 18 September 2007
Available online 26 September 2007
Editor: R.W. Carlson

Abstract

An extensive dataset of ocean island basalt (OIB) compositions highlight that their titanium (Ti) contents are generally too high to be derived from melting of a peridotitic mantle. Even vanishingly small degree melts of a primitive mantle source have insufficient Ti to reproduce the compositions of many OIB. A Ti-enriched material is thus a necessary additive to many OIB sources. Of the enriched components commonly invoked to explain the range in OIB radiogenic isotopic signatures, only the addition of small amounts (~1–10%) of recycled mafic crust is compatible with all geochemical constraints. Since such mafic crust starts melting deeper than its host peridotite, small degree melts formed beneath thick lithosphere will preferentially sample this enriched heterogeneity. This is compatible with the observation that the most Ti rich OIB also have the most enriched and variable signatures in terms of radiogenic isotope ratios. However, recycled mafic crust itself is insufficiently extreme isotopically to be able to account for the full range of isotopic ratios in OIB, therefore further, associated components (e.g. sediments, metasomatic veins) seem necessary in some cases.

Keywords: Ocean Island Basalts; titanium; recycled oceanic crust; radiogenic isotopes

1. Introduction

The variable but 'enriched' geochemical nature of ocean island basalts (OIB) relative to mid ocean ridge basalts (MORB) has long been recognized (e.g. Gast et al., 1964). This contrast in compositions between magmas from intra-plate and constructive margin settings potentially provides a key constraint on dynamic models of the Earth's interior. For example, Chase (1981) and Hofmann and White (1982) used radiogenic isotope evidence to infer recycling of subducted slabs to generate deep, enriched mantle sources of OIB. Subsequently, similar models have been widely invoked to account for the full range of isotopic signatures observed in OIB. This is a plausible and appealing concept but is not without detractions (e.g., Halliday et al., 1995; Niu and O'Hara, 2003).

Characterizing OIB sources using radiogenic isotope compositions has the advantage that these isotope ratios should be negligibly influenced by the melting process and subtle variations in erupted basalts can be confidently related to source variability. However, a problem lies in interpreting rather small, albeit analytically significant, isotopic variations. A wide range of processes from recycling to metasomatism can produce parent–daughter fractionations that, with time, may

* Corresponding author. Tel.: +44 117 954 5421; fax: +44 117 925 3385.
E-mail address: J.Prytulak@bristol.ac.uk (J. Prytulak).
[1] Tel.: +44 117 954 5421; fax: +44 117 925 3385.

0012-821X/$ - see front matter © 2007 Elsevier B.V. All rights reserved.
doi:10.1016/j.epsl.2007.09.015

evolve into similarly perturbed isotopic ratios. Moreover, there is a trade off between the age and magnitude of parent–daughter fractionation in generating a given isotopic signature. Not surprisingly, such ambiguities have given rise to a number of different models used to account for the same observed isotopic variations.

Additional constraints on the nature of enrichment in OIB sources, independent of trace elements or isotopic ratios, would therefore be valuable (e.g. Sobolev et al., 2005, 2007). Non-isotopic approaches, however, require knowledge of the poorly constrained melting process to invert erupted compositions. In this contribution we circumvent the need to calculate accurately the effects of partial melting by exploring the notion that the abundance of Ti in many OIB exceeds any values that might result from melting of simple peridotite sources (e.g., Dasgupta et al., 2006; Frey et al., 1994; Hémond et al., 1994; McKenzie and O'Nions, 1991). We find that even primitive mantle compositions, melted to vanishingly small degrees of melt cannot account for the magnitude of the TiO_2 concentrations in many OIB. Accounting for this 'excess' abundance of Ti then provides us with a novel means of distinguishing possible sources of enrichment.

2. Melting beneath ocean islands

The utility of Ti in probing OIB source composition stems from its well-characterized behavior during mantle melting. Indeed, we were initially interested in using Ti to derive the degrees of partial melting represented by ocean island basalts in an analogous manner to that used by Klein and Langmuir (1987) for MORB. The key feature of this approach is to invert the melt concentration of a moderately incompatible element. Since moderately incompatible elements are little influenced by metasomatism, via small degree melts, their possible source compositions are relatively well constrained. The major elements Na and Ti both have behaviors during mantle melting that can be classified as moderately incompatible and as major elements there are abundant data available.

The melting processes beneath ocean islands are more variable and less well understood than those beneath ridges (e.g., Klein and Langmuir, 1987; Bryan and Dick, 1982; McKenzie and Bickle, 1988; Langmuir et al., 1992). Perhaps most importantly for ocean islands, the oceanic lithosphere on which they lie progressively thickens with distance away from ridge axis. This lithosphere acts as a barrier to the vertical motion of upwelling mantle and, since most mantle melting is believed to be driven by adiabatic decompression, this brings melting to a halt. For upwelling mantle of a constant potential temperature, the influence of variable thickness lithosphere will result in larger degree, shallower melts beneath thin lithosphere and smaller degree, deeper melts beneath older, thicker lithosphere (Fig. 1). This dominant control on melt composition is consistent with systematic variations in silica undersaturation and rare earth element fractionations in OIB overlying lithosphere of different ages (Ellam, 1992; Haase, 1996; McBirney and Gass, 1967).

The wide variability in the mean depth of melting beneath different ocean islands precludes the effective use of Na abundances in OIB to determine their degrees of melting, in contrast to the MORB case. This results from the marked increase in compatibility of Na in clinopyroxene with increasing pressure (e.g., Blundy et al., 1995; Kinzler, 1997; Langmuir et al., 1992; Litvin and Gasparik, 1993). The increase in concentration of Na that should result from smaller degrees of melting beneath thicker lithosphere is counter-acted by its decrease in incompatibility at higher pressures. Thus the sensitivity of Na concentrations to the degree of melting in OIB is greatly diminished and strongly dependent on calibrations of the effect of pressure on its partitioning into clinopyroxene.

Such complexity in the use of Na to assess the degree of melting in OIB can be usefully illustrated with an example from the Azores. The islands of the Azores archipelago lie at variable distances from the mid-Atlantic ridge. We look at two islands that lie atop oceanic crust of different age and therefore lithosphere of different model thickness, namely Pico (~10 Ma, 35 km thick, Cannat et al., 1999) and São Miguel (53 Ma, 80 km thick, Searle, 1980), see Fig. 1. These islands provide a good comparison since the most westerly lavas of São Miguel, from the Sete Cidades volcanic centre, have very similar radiogenic isotopes to lavas from Pico Island (e.g. Elliott et al., 2007), thus removing uncertainties related to different mantle sources. Since Pico lies much closer to the mid-Atlantic ridge, its source should undergo greater amounts of decompression to produce higher degrees of melt than the isotopically similar mantle beneath São Miguel. Yet, Pico lavas have higher abundances of sodium than comparably differentiated São Miguel lavas (Fig. 1), which is the opposite of expectations if sodium behaves as a simple, moderately incompatible element (as in MORB genesis). Notably, the titanium contents of lavas from Pico are lower than São Miguel, as would be anticipated for a moderately incompatible element in higher degree melts (Fig. 1). Thus Ti, rather than Na,

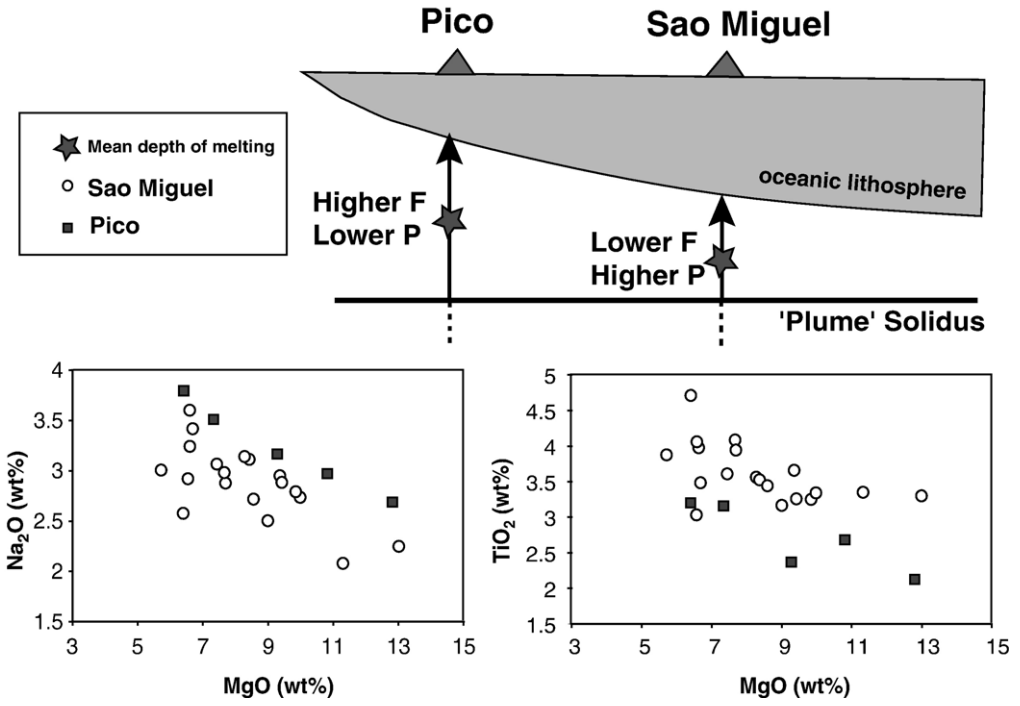

Fig. 1. Schematic representation of the melting regime beneath the Azores archipelago. Pico Island lies on thinner lithosphere closer to the mid-Atlantic ridge than São Miguel. Plots of Na_2O versus MgO show that although Pico is comprised of larger degree melts, they have higher Na_2O contents than the smaller degree melts of São Miguel. This behaviour reflects the decreasing incompatibility of sodium with depth. In contrast, TiO_2 has higher abundances in the lower degree melts of São Miguel, therefore behaving in the expected manner for a moderately incompatible element. Major element data from Elliott et al. (2007).

appears to be the moderately incompatible element of choice when examining OIB melting.

3. Behavior of Ti during melting and fractionation of OIB

We originally wished to use the Ti concentrations in OIB to infer the degrees of melt they represent. As evident below, it was not possible to model the Ti contents of OIB as a result of simple melting of peridotite. We thus use the data to infer minimum Ti source compositions of OIB, assuming a range of melting degrees. In either case, however, it is initially necessary to quantify the primary TiO_2 contents of OIB and Ti behavior during mantle melting.

3.1. Fractionation Paths

In order to assess the primitive TiO_2 contents of OIB suites and assign a 'reference' value that reflects this composition, we compiled major element data from the GEOROC database (http://georoc.mpch-mainz.gwdg.de/georoc/) and other recent relevant literature (see Table 1 and supplementary information). Analyses are dominantly whole rock measurements but, where available, glass compositions are included as these typically more faithfully record liquid compositions. We have concentrated on the major ocean islands that have sufficiently numerous analyses to illustrate differentiation trends. This has also provided coverage of the full range of isotopic 'endmembers' (e.g., Zindler and Hart, 1986) and representatives from most of the major hotspots.

To investigate primary TiO_2 contents in OIB, we need to account for variable amounts of fractional crystallization. Klein and Langmuir (1987) introduced the now widely used method of correcting oxides such as Na_2O and FeO back to a reference magnesium concentration (8 wt.% MgO). Similarly we derive a reference TiO_2 value from the trend of the liquid line of descent (LLD), but we estimate a minimum primitive TiO_2 and its uncertainty using a range of more mafic compositions. Fig. 2a shows a generalized diagram of a LLD, typical of many OIB. Fractionation along an olivine control line will gradually increase TiO_2 contents up to an inflection point where there is a drastic increase in TiO_2 at the onset of plagioclase fractionation (Fig. 2a, usually 8–10 wt.% MgO). More

Table 1
Compilation of Global OIB dataset

OIB	Number of analyses	Number of analyses	Reference TiO_2
	WR	Glass	
Iceland	2233	596	1.0 (0.2)
Mauna Loa	585	103	1.8 (0.2)
Galapagos	639	16	1.8 (0.3)
Oahu	587	73	1.9 (0.4)
Kilauea	2033	872	2.0 (0.2)
Mauna Kea	987	585	2.1 (0.2)
Reunion	587	42	2.1 (0.3)
Cook-Austral	431	8	2.2 (0.4)
St. Helena	127	0	2.4 (0.3)
Pitcairn	93	0	2.5 (0.3)
Samoa	219	97	2.7 (0.3)
Society Islands	356	13	2.8 (0.3)
Gran Canaria, Canary Is.	651	26	3.0 (0.3)
Cape Verde	378	0	3.0 (0.3)
Sao Miguel, Azores	204	0	3.0 (0.3)
La Palma, Canary Is.	381	13	3.0 (0.3)
Tristan da Cunha	127	0	n.d

Data set is compiled mainly from the GEOROC Database (see supplemental information for individual determinations and a full dataset). Errors on estimated reference values are given in parentheses, n,d: not determined.

alkalic lavas have clinopyroxene cotectic with olivine during early differentiation and plagioclase appears on the liquidus after the dramatic decrease in TiO_2 that marks the saturation of titan-magnetite (see Appendix A in supplemental information). In either case, the initial slope of the LLD on a MgO vs TiO_2 plot is shallow and so any uncertainty in the primary MgO content of the magma has little effect on our estimated reference TiO_2. Nevertheless, reasonable values of primary MgO contents need to be assessed.

Primary magmas generated from the anomalously vigorous Hawaiian plume are likely the hottest and therefore most MgO rich of all OIB but generally do not exceed 16 wt.% MgO (Norman and Garcia, 1999). Therefore we consider any more magnesian lavas are likely to be accumulative. Subsequently, for OIB other than Hawaii, we estimate the reference TiO_2 value from the slope of an olivine control line along the bottom of the data array between 10 and 15 wt.% MgO. The error on this value is derived by the slope of the olivine control line (Fig. 2b). Hawaiian lavas have very well-defined LLD (see Figs. S1–S4, supplemental information). For these locations, we take the reference TiO_2 content at 16 wt.% MgO, and estimate the error by the width of the data array at this point. Finally, we compare other available independent estimates on primary MgO and TiO_2 contents with our TiO_2 reference values. For example, Fig. 2b shows a well-defined LLD from Reunion showing our TiO_2 'reference' value compared to an estimate of primary TiO_2 derived by an entirely different approach are in good agreement. For a complete discussion of the determination of reference values and each OIB LLD, see the Appendix in the supplemental information.

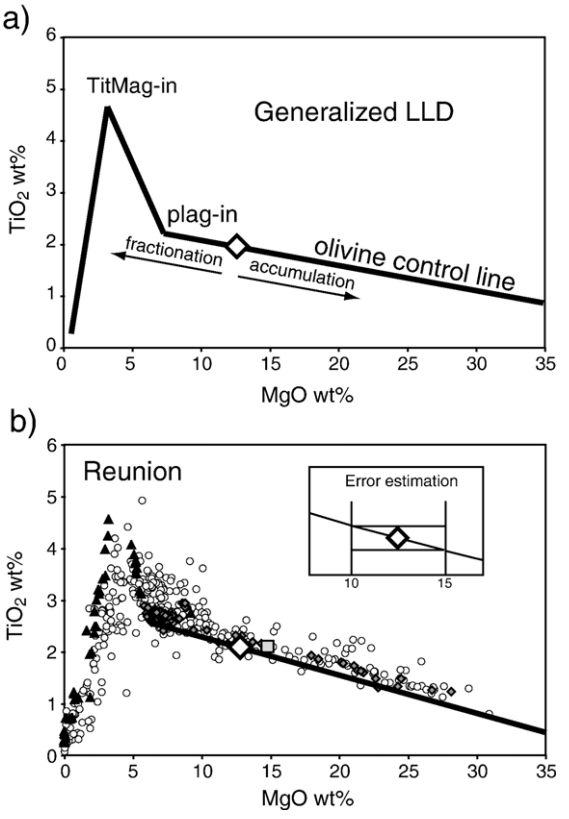

Fig. 2. a) Cartoon of a typical liquid line of descent for a primary OIB composition in which plagioclase is cotectic before titan-magnetite saturation. b) MgO wt.% versus TiO_2 wt.% for Reunion Island. Grey diamonds are whole rock analyses from post 1931 historical activity of Piton de la Fournaise volcano. Open circles are whole rock analyses that are older than 1931, or of uncertain affinity and black triangles are glass analyses. We determine a reference TiO_2 value of 2.1 ± 0.3 from the olivine control line between 10 and 15 wt.% MgO. Albarède and Tamagnan (1988) estimated a primitive MgO content of 9 wt.% for post 1931 lavas, determined by fractionation regression lines of Ni and MgO abundances. The value of 9 wt.% MgO corresponds to approximately 2.5 wt.% TiO_2. Fretzdorff and Haase (2002) determined that the most primitive melt had an MgO content of approximately 14 wt.% from the intersection of mixing trends in major element space. Their inferred near primitive sample 13 DS-2 has a TiO_2 content of 2.1 wt.%, in good agreement with our reference value. For a full assessment of the reference TiO_2 values derived for other OIB used in this study, see the supplemental information.

3.2. Modeling Ti behavior during mantle melting

After establishing our reference TiO_2 values (Table 1), we attempt to account for their magnitudes. To do this we set up a simple melting model. OIB melting likely begins in the garnet peridotite stability field, as evident from geochemical parameters such as relative HREE abundances. However, melting can continue into the spinel stability field. Therefore, we focus on two endmember scenarios: melting in the garnet stability field, and melting in the spinel stability field. In this way, we can assess the dependence of our model on the mineralogical and compositional changes as melting proceeds to shallower depths. The key variables that need to be addressed for both cases are the partition coefficients of Ti between mantle minerals and melt.

3.2.1. Titanium partitioning in peridotite assemblages

Melt-solid partitioning is critically dependent on ambient pressure, temperature, and the compositions of the melt and especially the mineral phases (see Wood and Blundy, 2003 for a recent review). It is clearly inappropriate to assume that partition coefficients remain constant throughout the melting process when these fundamental parameters vary. By examining the partitioning of Ti during both spinel peridotite and garnet peridotite melting, we can determine both the magnitude and sense of change between these two endmember scenarios. To remove the uncertainty introduced by mixing data from different experimental conditions, we further focus on studies that have analyzed all or most of the major mantle phases in the same experiment. Ideally, we also require experiments that compositionally approximate small degree near solidus mantle melts. The studies of Kinzler (1997), McDade et al. (2003) and a dataset from McDade, Blundy, and Wood and Dalton (unpublished, Blundy writ. comm., 2006) performed within the garnet stability field in an analogous manner to McDade et al. (2003), best meet our requirements. Kinzler (1997) performed experiments on mixtures of natural peridotite and basalts to approximate small degree melts while retaining large experimental melt fractions. The more recent approach of McDade et al. (2003) employs an 'iterative sandwich' technique to ensure equilibrium between their analyzed phases and natural peridotite, whilst still approximating small degree melts.

For melting in the spinel peridotite stability field, we chose the partition coefficients of experiment L125 from Kinzler (1997). We employ data from Kinzler (1997) instead of McDade et al. (2003) simply because it includes spinel partitioning data, otherwise both studies yield similar bulk partition coefficients. For melting in the garnet stability field, we chose experiment R84-9 from the dataset of McDade, Blundy, Wood, and Dalton. Some of the higher pressure experiments of Kinzler (1997) contain garnet but the study concentrated mainly on spinel peridotite and the transition to garnet peridotite. Walter (1998) present extensive data from high pressure melting experiments, but the focus of this work was komatiite genesis, so the permutations of degree and pressure of melting are inappropriate for OIB melting. For example, the lowest pressure (3 GPa) runs of Walter (1998) are compatible with the depth of OIB melting but represent such large degrees of melting (~20%) that garnet is exhausted in the residue. The recent experimental work of Dasgupta et al. (in press) determined self-consistent sets of $D_{Ti}^{mineral/melt}$ at 3 GPa for carbonated natural peridotite. The resulting $D_{Ti}^{mineral/melt}$ values determined for peridotite with 1 wt.% CO_2, which is significantly higher than realistic mantle concentrations, yield $\bar{D}_{Ti}$ no lower than our calculated value based on anhydrous experiments (see Dasgupta et al., in press, experiment A471, and the supplemental information). However, experiments that contain 2.5 wt.% CO_2 have $D_{Ti}^{cpx/melt}$ (~0.1) and $D_{Ti}^{garnet/melt}$ (~0.13) significantly smaller than any other literature experiments at the same pressures and temperatures, including Walter (1998). Therefore, we note that high concentrations of CO_2 might be effective in lowering $D_{Ti}^{mineral/melt}$.

3.2.2. Systematics of D_{Ti} in individual mantle phases

Although we have specifically chosen values of $D_{Ti}^{mineral/melt}$ from experiments most relevant to OIB melting, we also wish to consider the appropriateness of these values from a wider understanding of Ti partitioning available from experiments performed over a greater range of pressure and temperature. Fig. 3 shows an overview of Ti partitioning in major mantle phases during volatile-free peridotite melting focusing on experiments in the pressure range of ~1–3 GPa and ~1200–1500°C. It is clear that the minerals exerting the most control over the titanium bulk partition coefficient ($\bar{D}_{Ti}$) are clinopyroxene and garnet. Our preferred values (indicated by arrows in Fig. 3) are typically not extreme. Whilst our chosen value of $D_{Ti}^{cpx/melt}$ for melting in the spinel stability field is towards the higher values, this is entirely appropriate given the well constrained systmatics of Ti partitioning into clinopyroxene that we discuss below.

Lundstrom et al. (1998) noted that $D_{Ti}^{cpx/melt}$ (and the partitioning behavior of the other HFSE) is strongly related to the mineral's aluminum content. Subsequent studies confirmed this observation (e.g., Dasgupta et al.,

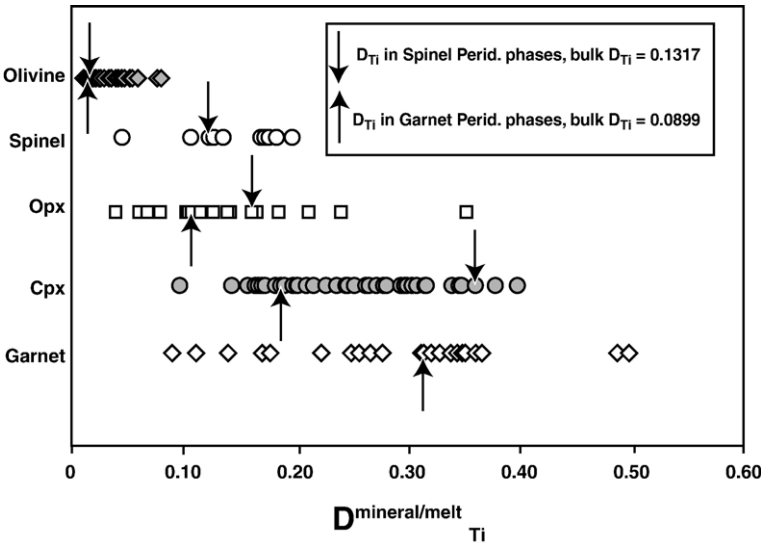

Fig. 3. A compilation of $D_{Ti}^{mineral/melt}$ for major mantle phases from peridotitic experiments in the range of 1-3 GPa. Mineral partition coefficients were compiled from (Kinzler and Grove, 1992; Kinzler, 1997; McDade et al., 2003; Parman and Grove, 2004; Salters and Longhi, 1999; Walter, 1998; Wood and Blundy, 2003). Arrows indicate the values used in this study for minerals in spinel (down) and garnet (up) peridotite assemblages. The values chosen for garnet peridotite are from experiment R84-9 from (McDade, Blundy, Wood and Dalton unpublished data) and are: $D_{Ti}^{cpx/melt}=0.173$, $D_{Ti}^{opx/melt}=0.125$, $D_{Ti}^{gnt/melt}=0.315$. $D_{Ti}^{ol/melt}$ was not reported for this experiment, so we adopt a value of 0.02, consistent with the higher pressure experiments of Kinzler (1997). Values for spinel peridotite are from experiment L125 of Kinzler (1997) and are: $D_{Ti}^{ol/melt}=0.031$, $D_{Ti}^{cpx/melt}=0.361$, $D_{Ti}^{opx/melt}=0.186$, $D_{Ti}^{sp/melt}=0.124$. For a compilation of $D_{Ti}^{mineral/melt}$ from key studies, see the supplemental information.

2006; Hill et al., 2000; Longhi, 2002). Specifically, the aluminum in the tetrahedral site of clinopyroxene is positively correlated with $D_{Ti}^{cpx/melt}$. Wood and Blundy (2003) provide an empirical relationship between $D_{Ti}^{cpx/melt}$ and aluminum in the tetrahedral site.

$$\log D_{Ti}^{cpx/melt} = -0.838 + 2.71Al^{iv} \quad (1)$$

Eq. (1) illustrates that composition alone can be used to estimate $D_{Ti}^{cpx/melt}$ and reproduces our values within a factor of two. However, the composition of clinopyroxene in a mantle assemblage is related to the ambient pressure and temperature, which further influence partitioning. To explore more fully the consequent P–T relations of $D_{Ti}^{cpx/melt}$, we compiled experimental data relevant to OIB genesis from peridotitic sources (Fig. 3 and the higher pressure experiments of Walter, 1998 to improve the regressions). We then performed a step-wise linear regression on the dataset using the functional form suggested by Hill (2000) to obtain the following equation for $D_{Ti}^{cpx/melt}$ along the mantle solidus:

$$R\ln D_{Ti}^{cpx/melt} = 75.865 - 3.035P - 0.052T - 0.014P^2 \quad (2)$$

It is evident that over the range of interest for OIB generation (1.5 to 3 GPa), there is little pressure dependence of $D_{Ti}^{cpx/melt}$ (Fig. 4a). Blundy et al. (1995) similarly parameterized $D_{Na}^{cpx/melt}$, which is also shown for comparison. $D_{Na}^{cpx/melt}$ shows a marked increase with increasing pressure, which was invoked above to account for the apparently anomalous behavior of Na between Pico and São Miguel suites in the Azores (Fig. 1).

A recent compilation of both peridotitic and pyroxenitic experiments by Pertermann and Hirschmann (2003) suggested that $D_{Ti}^{cpx/melt}$ is more sensitive to temperature than pressure changes. Our compilation from peridotitic experiments also indicates a negative temperature dependence on $D_{Ti}^{cpx/melt}$ (Fig. 4b). Temperature effects on $D_{Ti}^{cpx/melt}$ are best illustrated by the study of Walter (1998), which used elevated temperature and large melt fractions and shows some of the lowest $D_{Ti}^{cpx/melt}$ in the literature (see supplemental information).

We can use Eq. (2) to compare the calculated $D_{Ti}^{cpx/melt}$ at the P-T conditions of our chosen experiments with the measured values. For experiment L125 of Kinzler (1997), the calculated value is 0.37, which compares well with the measured value of 0.36. Experiment R84-9 also fits well with Eq. (2), having measured and calculated values of 0.173 and 0.177, respectively. Significantly, our regression of a larger number of experiments is consistent with the specific values of $D_{Ti}^{cpx/melt}$ we use from experiments that contain all appropriate phases at mantle solidus conditions.

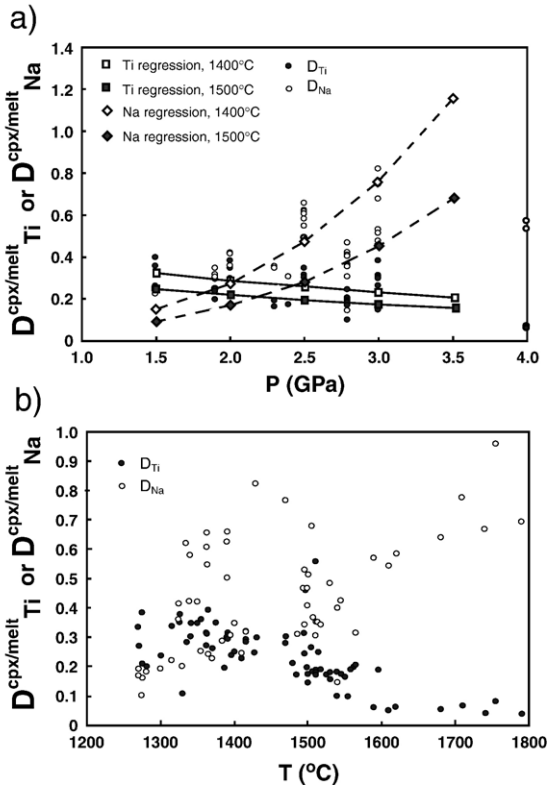

Fig. 4. Contrasting partitioning behavior of Na and Ti with pressure and temperature. a) Partition coefficients versus pressure close to peridotite solidus. $D_{Na}^{cpx/melt}$ shows a marked increase with increasing pressure whilst $D_{Ti}^{cpx/melt}$ remains relatively constant over the interval of interest for OIB melting (1.5 to 3 GPa). Regression equations for $D_{Na}^{cpx/melt}$ are from Blundy et al. (1995), and the form of the regression equation for $D_{Ti}^{cpx/melt}$ is from Hill (2000), using a step-wise linear regression performed on a filtered dataset (see text for discussion). b) Partition coefficients of Na and Ti in clinopyroxene as a function of temperature. $D_{Ti}^{cpx/melt}$ decreases with increasing temperature, whilst $D_{Na}^{cpx/melt}$ increases, although the increase may result from the higher pressures that accompany the higher temperatures. Data is from the same sources as Fig. 3, but also include the experiments of Walter (1998) to define the regressions better at higher pressures.

When present, garnet can exert considerable influence over $\bar{D}_{Ti}$ (Fig. 3). Fortunately, $D_{Ti}^{gnt/melt}$ in pyropic garnet in peridotitic assemblages appears to remain relatively constant over a wide range of temperatures and pressures (e.g. Pertermann and Hirschmann, 2003; Walter, 1998). Compositional effects appear to be the greatest influence on garnet partitioning behavior. For example, in one of the few studies of compositional controls on Ti partitioning into garnet, van Westrenen et al. (1999) show that Ti can be an order of magnitude more compatible in grossular-rich (Ca) garnets than pyrope-rich (Mg) garnets. It should be noted, however, that the van Westrenen et al. (1999) experiments were performed on garnet compositions in a pure system and well outside normal peridotitic garnets.

Titanium does not significantly partition into olivine. The value we use for olivine ($D_{Ti}^{ol/melt}=0.02$) is lower than average, but not extreme. Orthopyroxene has a higher $D_{Ti}^{mineral/melt}$ than olivine, but generally not as high as cpx or garnet (Fig. 3). Our values for $D_{Ti}^{opx/melt}$ of 0.186 (spinel peridotite) and 0.125 (garnet peridotite) are close to averages from a wider dataset. $D_{Ti}^{sp/melt}$ is similar to $D_{Ti}^{opx/melt}$. Titanium partitioning into opx and spinel has not been studied in great detail, however, they show somewhat limited variability from the experimental data available and so emphasis is placed on their derivation from self-consistent datasets at appropriate conditions.

We use modal mineral abundances for spinel peridotite from Kinzler (1997) to derive our $\bar{D}_{Ti}$. Using modes of 53%ol+27%opx+17%cpx+3%sp, and $D_{Ti}^{ol/melt}=0.031$, $D_{Ti}^{opx/melt}=0.186$, $D_{Ti}^{cpx/melt}=0.361$, $D_{Ti}^{sp/melt}=0.124$ (Kinzler, 1997), we calculate $\bar{D}_{Ti}=0.132$ for spinel peridotite. For garnet peridotite we use modes of 53%ol+16%opx+27%cpx+4%gnt (Walter, 1998) and $D_{Ti}^{opx/melt}=0.125$, $D_{Ti}^{cpx/melt}=0.173$, $D_{Ti}^{gnt/melt}=0.315$ from experiment R84-9 of McDade, Blundy, Wood, and Dalton (Blundy, writ. com, 2006). $D_{Ti}^{ol/melt}$ was not reported for this experiment, so we use a value of 0.02 to be consistent with the higher-pressure experiments of Kinzler (1997). These partition coefficients yield $\bar{D}_{Ti}=0.0899$ for garnet peridotite. It is worth noting that the small modal abundance (4%) of garnet in peridotite at 3 GPa (Walter, 1998) and increasing this value, as appropriate for melting at higher pressure will cause an increase in the $\bar{D}_{Ti}$ value.

3.2.3. Melting model

To model the behavior of Ti during OIB melting, we use simple equilibrium batch melting. Melting likely proceeds in a more 'dynamic' fashion (e.g. Langmuir et al., 1977). However, batch melting recovers the behavior of incompatible elements well, even if the true process is more complex (see Ribe, 1985; Richter, 1986). We examine a non-modal melting scenario using the notation of Shaw (1970):

$$\frac{C_l}{C_o}=\frac{1}{D_o+F(1-P)} \tag{3}$$

where C_l is the concentration of the element of interest in the liquid, C_o is its initial concentration in the source, D_o is its bulk partition coefficient in the initial mineral assemblage, P is the bulk partition coefficient of the components entering the melt, and F is the degree of melting.

4. Model results

We use our melting model to calculate the minimum Ti source compositions required to generate different reference OIB compositions (Fig. 5). The degrees of melting represented by OIB are not well defined, however, they are widely believed to be less than the mean 10% melting that produces MORB (Klein and Langmuir, 1987; McKenzie and Bickle, 1988). Even melts from the vigorous Hawaiian hotpot are thought to be ~5% (e.g., McKenzie and O'Nions, 1991; Watson and McKenzie, 1991). Given this uncertainty, we illustrate the problem using a range in model degrees of melting, from values as high as suggested for MORB (~10%) to infinitesimally small (0%). The latter provides a maximum possible enrichment of Ti during melting and hence minimum value of Ti content in the OIB source. These model values of Ti content of the OIB sources can then be compared to our reference values.

The source concentration of Ti in a peridotitic mantle should lie between primitive mantle (1300 μg/g, Sun and McDonough, 1989) and depleted MORB mantle (700 μg/g, Workman and Hart, 2005). Melts derived from the oceanic mantle typically show radiogenic isotopic signatures that indicate long-term source depletion in incompatible elements. Thus OIB would not be anticipated to have source Ti contents as high as primitive mantle values. For example, the mantle has experienced continental extraction and might also be influenced by the presence of an early-formed enriched hidden reservoir (Boyet and Carlson, 2005). Both of these processes should lower the Ti content of the residual mantle reservoir. As a moderately incompatible element such depletions are not huge for Ti, but a primitive mantle composition nevertheless provides a clear maximum source Ti concentration for a simple peridotitic mantle. It is also worth noting that, as a refractory, lithophile element, the terrestrial budget of Ti is well constrained.

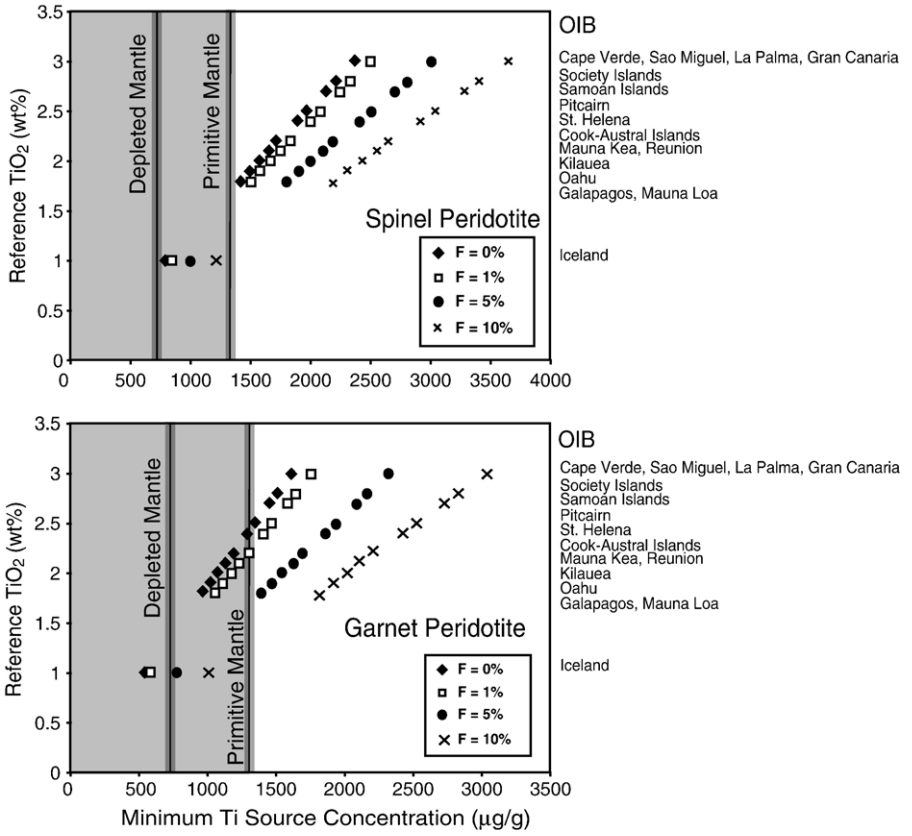

Fig. 5. Reference TiO_2 contents of our global OIB dataset (Table 1) versus the minimum source Ti concentration required to produce such primitive magmas for a range of degrees of melting within a) the spinel peridotite stability field and b) the garnet peridotite stability field. The shaded area represents permissible concentrations for any likely peridotitic mantle source up to primitive mantle concentrations (~1300 μg/g, Sun and McDonough, 1989). Depleted mantle Ti concentrations is also marked (~700 μg/g, Workman and Hart, 2005). The melting reaction used to calculate F>0 for garnet peridotite at 3 GPa: 0.07ol+0.68cpx+0.25gnt=0.84liq+0.16opx (Walter, 1998) and for spinel peridotite at 1.5 GPa: 0.19ol+0.80cpx+0.13sp=0.13opx+1.0liq (Kinzler, 1997). See text for further details about the melting model.

Surprisingly, many calculated OIB source concentrations plot to values greater than the primitive mantle (Fig. 5). An additional, Ti-enriched component is evidently required in nearly all OIB sources studied, regardless of their isotopic character. It is important to stress that this is true of many OIB, even in the extreme scenario of generating lavas from a primitive mantle source melted to infinitesimally small degrees (Fig. 5). Clearly at finite degrees of melting for more plausibly depleted sources, the amount of source Ti enrichment required becomes even more marked. Hawaiian lavas can be produced from a primitive mantle with 0% to 3% melting. However, as previously discussed, there are many other lines of evidence that suggests the Hawaiian melts are derived from higher degrees of melting (~5%) and from a depleted mantle source.

Iceland is a notable exception and does not clearly require additional Ti in its source (Fig. 5). Icelandic lavas, however again represent significantly larger degree of melt than typical OIB because of their location on the mid-Atlantic ridge. It is possible that Iceland also needs enriched components, but this case requires a more careful consideration of individual eruptive suites, appropriate degrees of melting, and residual mineralogy that is not necessary in other locations. Although an interesting topic for future work, we will not further consider these issues here.

Having discussed the key controls on partition coefficients in the previous section, we believe our carefully assessed values are appropriate for peridotite melting and, if anything, are at a conservatively low end of the possible range. Our method of determining a reference TiO_2 value also generates conservatively low values, again emphasizing the need for TiO_2 enrichment in the mantle source. Fig. 5b illustrates model values calculated with a garnet source suitable for most OIB. As melting proceeds from the garnet stability field to the spinel stability field, $\bar{D}_{Ti}$ increases (Figs. 3 and 5a). Thus if we used partition coefficients of the spinel stability field this would only reinforce our arguments. To derive $\bar{D}_{Ti}$ low enough (<0.06) to reconcile the TiO_2 contents of OIB with plausible amounts of melting (~1%) would unreasonably require that clinopyroxene and garnet were absent from the source. Therefore, we are confident that our model results, shown in Fig. 5, provide robust constraints.

5. Discussion

We have shown that a Ti-rich component is required in the source of OIB. Previous studies using trace elements and isotopic systems have long identified the need for additional enriched components in the OIB source. As discussed above, however, trace elements and isotopic ratios can be equivocal in their identification of the processes causing heterogeneity. Below, we systematically examine commonly invoked mechanisms of enrichment (Table 2) to determine if they can account for the elevated TiO_2 contents of the global OIB dataset. Perhaps surprisingly, the requirement of high TiO_2 contents in the OIB source transpires to be a highly distinctive fingerprint of the nature of the enrichment process.

5.1. The lithospheric mantle and metasomatism

Enrichment of the mantle by small degree, 'metasomatic' melts has been a popular mechanism to generate some of the more extreme isotopic and trace element signatures seen in OIB (e.g., Halliday et al., 1995; McKenzie and O'Nions, 1983, 1991, 1995; Niu and O'Hara, 2003; Sun and McDonough, 1989; Workman et al., 2004). The role of the sub-continental lithospheric mantle (SCLM) in OIB genesis was discussed conceptually by McKenzie and O'Nions (1983, 1995). More specifically, the composition of some Atlantic OIB have been isotopically related to fragments of SCLM from Pangea, broken off during the opening of the Atlantic (e.g., Hawkesworth et al., 1986). More recently the role of metasomatised oceanic lithospheric mantle as a

Table 2
Titanium concentrations of possible contributors to OIB magmatism

Material	TiO_2 (wt.%)	Reference
SCLM	0.001 to 0.1	Beyer et al., 2006; Hellebrand et al., 2002
DMM	0.1195	Workman and Hart, 2005
Primitive Mantle (PM)	0.217	Sun and McDonough, 1989
GLOSS	0.62	Plank and Langmuir, 1998
Upper Continental Crust	0.64	Rudnick and Gao, 2004
Terrigenous Sediment	0.726	Prytulak et al., 2006
Lower Crust	0.82	Rudnick and Gao, 2004
Pelagic Clay (Tonga)	0.893	Plank and Langmuir, 1998
MORB	1.268	Sun and McDonough, 1989
Eclogite	0.44 to 2.77 (avg. 1.46)	Becker et al., 2000
AOC (ODP Site 801)	2.67	Kelly et al., 2003
Silica-undersaturated melt of a carbonated eclogite	19	Dasgupta et al., 2006

recycled component in enriched mantle sources has also been proposed (Niu et al., 2002; Niu and O'Hara, 2003; Workman et al., 2004).

There are several styles of metasomatism recorded in mantle xenoliths derived from SCLM (e.g., Kempton, 1987) potentially giving rise to a wide range of isotopic compositions and highly incompatible element abundances. In general terms however, such processes represent the enrichment of a depleted lithosphere with small degree melts that strongly influence the budget of highly incompatible elements (see Kempton, 1987). Similarly, in the oceanic environment, the geochemical signatures of small degree melt impregnation are most pronounced in highly incompatible element abundances (e.g., Hellebrand et al., 2002; Johnson et al., 1990; Niu, 1997). However, even samples with considerable degrees of 're-fertilization' by metasomatic melts do not show correspondingly enriched Ti concentrations and can be quite Ti-depleted (e.g., Beyer et al., 2006; Hellebrand et al., 2002). This is consistent with Ti-depletion during the initial, lithosphere forming melting event. TiO_2 concentrations less than 0.05 wt.% (Table 2) are consistent with model calculations of fractional removal of approximately 10% melt from a primitive mantle source. Whilst addition of metasomatic veins can counter-act this initial depletion for the most highly incompatible elements, this is not the case for moderately compatible elements such as Ti. Indeed, the immunity of moderately incompatible elements to small degree melt metasomatism is one of their main utilities (Klein and Langmuir, 1987). Thus the lithospheric mantle is likely depleted in Ti compared to the primitive mantle. A possible exception is when the mantle is modally metasomatised as the result of extensive melt impregnation or accumulation of cumulates (e.g., Pilet et al., 2005). This case is thus hard to distinguish from the simple addition of basaltic material to peridotite that we discuss later, but is volumetrically much less significant than recycling of mafic oceanic crust (see below).

5.2. Sediments and the continental crust

Sediments have been widely championed as the cause of enriched OIB signatures. An attractive version of this paradigm links the subduction of pelagic and terrigenous sediments to EMI and EMII sources, respectively (Weaver, 1991), although alternatives to sediment involvement have been proposed for both components (e.g., Elliott et al., 2007; McKenzie et al., 2004; Workman et al., 2004). We assess whether subducted sediments can reconcile the high Ti concentrations of our studied OIB. This task is helped considerably by the compilation of subducting sediment assemblages by Plank and Langmuir (1998). Since Ti is believed to behave conservatively during subduction, modern oceanic sediment compositions should provide a reliable estimate of the abundance of TiO_2 in a deep subducted component.

Pelagic and terrigenous subducting sediments have higher Ti concentrations than the primitive or depleted mantle (Table 2). The averaged Ti composition of subducting sediments is approximated by GLOSS (0.62 wt.% TiO_2; Plank and Langmuir, 1998), and is used in the example calculations here. We examine the effect on radiogenic isotope signatures of mixing sufficient sediment into an OIB source to account for its high Ti content. We use the Sm–Nd and Lu–Hf systems, which like Ti, should be little perturbed by the subduction process. Assuming São Miguel is produced by infinitesimally small degrees of melt of a source with primitive mantle Ti concentrations, ~10% sediment addition would be required to account for its elevated Ti abundance (Fig. 6). Such a large addition of either terrigeneous or pelagic sediment would result in extreme Hf–Nd isotopic compositions that are not observed (Fig. 6).

The upper continental crust has titanium concentrations similar to GLOSS and the same arguments apply as above. The lower continental crust holds more promise as a source of titanium in OIB. The lower continental crust is more mafic than the upper crust, reflecting, for example, the presence of underplated basalts. This material may delaminate and potentially be mixed into an OIB source. As in the case of modal metasomatism it is difficult to distinguish this scenario from recycling mafic oceanic crust. Again we stress that mafic oceanic crust is volumetrically more abundant and its return to the mantle is more clearly evident. Therefore we note that a component of mafic lower continental crust could account for elevated Ti in OIB, but examine the more obvious mafic oceanic crustal source as a viable source of Ti in the following section.

5.3. Recycled mafic oceanic crust

The Ti concentration of recycled mafic crust can be well estimated from the Ti content of MORB, as it is neither greatly influenced by subduction nor seafloor alteration (Table 2). Mafic oceanic crust (MORB) has sufficiently high Ti (7800 μg/g, Sun and McDonough, 1989) such that only ~1–10% bulk addition to a peridotitic OIB source is required to account for the high Ti abundances, an amount broadly consistent with

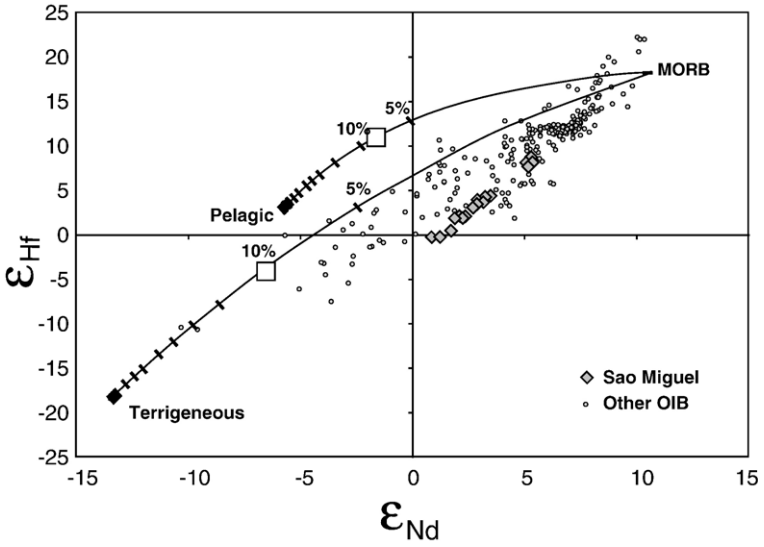

Fig. 6. Mixing relationships of the depleted mantle with terrigeneous and pelagic sediments Sediment addition large enough to sufficiently elevate OIB source Ti have profound, unobserved effects on the Hf-Nd systematics. Using two endmember compositions, addition of 10% terrigenous sediments or 8% pelagic sediment addition is required in a source with primitive mantle Ti concentrations, melted to infinitesimally small degrees to produce São Miguel lavas (reference TiO_2=3.0 wt.%). These sediment proportions are plotted as large white squares in the figure. Terrigenous sediment: Nd=30.41 μg/g, Hf=4.14 μg/g $^{143}Nd/^{144}Nd$=0.511945, $^{176}Hf/^{177}Hf$=0.282246, TiO_2=0.726 wt.% (Prytulak et al., 2006; sample 37-2-123-127). Pelagic sediment: Nd=48.17 μg/g, Hf=3.3 μg/g, $^{143}Nd/^{144}Nd$=0.512343, $^{176}Hf/^{177}Hf$=0.28285 (Vervoort et al., 1999; sample RC17-198), TiO_2=0.893 wt.% (Tonga, Plank and Langmuir, 1998). Primitive mantle: Nd=1.354 μg/g, Hf=0.309 μg/g (Sun and McDonough, 1989), $^{143}Nd/^{144}Nd$=0.513189, $^{176}Hf/^{177}Hf$=0.283311 (Salters, 1996; sample TK5-1). OIB data are from the compilation of Vervoort et al. (1999) plus addition data from São Miguel, Azores (Elliott et al., 2007).

the recent work of Sobolev et al. (2007). A mixing scenario between recycled crust and ambient peridotitic mantle is more complex than simple bulk addition since a mafic component will melt earlier and more extensively than surrounding peridotite during adiabatic decompression (Hirschmann and Stolper, 1996). Thus a mafic component will contribute disproportionately to any erupted melt, making the bulk estimate of 1–10% crustal involvement a maximum. However, our calculations shown in Fig. 5 were extreme values, used to emphasize the need for a component rather than a best estimate of the amount of additional Ti required. More reasonable parameters would then raise the amount of mafic crustal component required. We do not attempt to rigorously consider a full two-component melting model, but suggest that the trade-offs above make a percent level contribution of mafic crust to the OIB source a plausible initial estimate.

Recycled mafic crust, unlike sediment, is not greatly different in its radiogenic isotope composition from the ambient mantle. During MORB genesis, Sm–Nd fractionation is only slightly increased, Pb is preferentially lost compared during subduction, and minor ^{87}Sr is gained over ^{86}Sr during seafloor alteration. The U and Rb gained during seafloor alteration are subsequently dominantly lost during subduction dehydration (for a more detailed discussion see Stracke et al., 2003). Recycled crust might thus be anticipated to have more radiogenic Pb and slightly more enriched Sr and Nd isotopic compositions compared to the depleted upper mantle. Indeed, the bulk of OIB are distinguished from MORB by such general differences. The percent-level addition of recycled crust to most OIB might also account for the ubiquitous FOZO signature (Hart et al., 1992).

To explore further the consequences of crustal addition to a peridotitic mantle, we compare the Nd isotopic composition of crust of different recycling ages mixed with mantle ranging in composition from primitive to depleted. These results are compared to our inferred OIB source compositions in Fig. 7. As in Fig. 5, it is again reinforced that the elevated TiO_2 contents of most OIB cannot be generated from melting of a peridotitic mantle. Mixing lines between the primitive mantle, the depleted mantle, and crust of different recycling ages (0.5 Ga to 1.5 Ga) delineate a region where Nd isotopic compositions resulting from mafic crustal addition can reside. Some OIB lie distinctly outside this region towards more enriched (lower) Nd isotopic compositions than can be reconciled using our crustal component. These OIB localities often have sediments and/or metasomatic

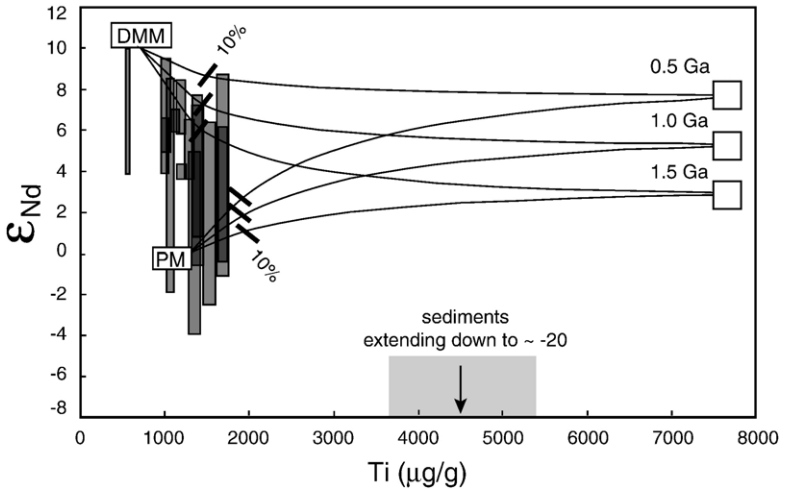

Fig. 7. Plot of ε_{Nd} versus Ti (µg/g) concentration showing mixing relationships (thin black lines) of differently aged oceanic crust with a peridotitic mantle of depleted and primitive endmember compositions. Individual OIB localities are represented by grey boxes encompassing required source concentrations calculated by assuming the erupted melts represent between 0 to 1% melts from the garnet stability field (see Fig. 5). Recycled mafic crustal ε_{Nd} are shown by white boxes. Mafic crust is assumed to have 1.3 wt.% TiO_2 (Sun and McDonough, 1989). Isotopic compositions are calculated assuming present day DMM has $^{143}Nd/^{144}Nd$ of 0.51315 and $^{147}Sm/^{144}Nd=0.1984$ whilst mafic crust has $^{147}Sm/^{144}Nd=0.2354$ (Sun and McDonough, 1989). Many OIB sources fall in a region that can be accounted for with ~1–10% eclogitic component in a depleted mantle source. A more isotopically enriched source is required for other OOIB and in a number of cases implies a component more enriched than putative primitive mantle. Sedimentary components generally plot to values <0 ε_{Nd} and their addition might account for OIB with more enriched ε_{Nd}. A general field for sedimentary components is shown using TiO_2 concentrations for GLOSS and pelagic sediments as endmembers (Plank and Langmuir, 1998) and a similar isotopic range as is Fig. 6.

enrichments invoked to explain their signatures (e.g., Samoa, São Miguel, Pitcairn, Society Islands). Moreover, as discussed above, the peridotitic host mantle in OIB sources is likely not primitive, therefore permissible Nd isotopic compositions from crust-mantle mixing are realistically restricted to even higher values of ε_{Nd}, further diminishing the ability of our simple model to account for the full range of isotopic signatures. Overall, it is appears that the amount of crust needed to satisfy the TiO_2 contents of OIB does not create the extreme isotopic compositions (Fig. 7).

There have been significant recent advances in experimental melting studies to reconcile the presence of recycled crust in OIB with major elements. These experiments involved such processes as melting mixtures of basalt and peridotite (e.g. Kogiso et al., 1998), anhydrous eclogite (e.g. Pertermann and Hirschmann, 2003; Pertermann et al., 2004), silica-deficient pyroxenite (e.g., Hirschmann et al., 2003; Kogiso et al., 2003) and carbonated silica-deficient garnet pyroxenite (Dasgupta et al., 2006). Most of these studies test variations on pyroxenite starting materials on the premise that melts derived from them are the sole contributor to OIB genesis. However, these melts will inevitably interact with the surrounding peridotite (e.g. Sobolev et al., 2005, 2007), which itself, must also melt. For example, Kogiso et al. (2003) could create OIB-like liquids from anhydrous, silica-deficient garnet pyroxenite at 5 GPa. However, the temperatures required would also mean that peridotite was above its solidus and would likely dilute any signature derived from the pyroxenite. This issue was addressed in the subsequent work of Dasgupta et al. (2006). By carbonating the anhydrous, silica-deficient garnet pyroxenite with 5 wt.% CO_2 the pyroxenite could be melted without fusion of the surrounding peridotite and produce a carbonatitic liquid and an immiscible, Ti-enriched silica-undersaturated liquid. This mechanism is attractive for the generation of extreme OIB compositions such as mellilites and nephelinites (Dasgupta et al., 2006). However, such a Ti-enriched liquid might more generally mix with peridotitic mantle or its melts to account for a fuller range of OIB compositions. We do not try to address in detail the full problem of eclogite melting and the subsequent reactions of these melts with surrounding peridotite.

5.4. Relationship of TiO_2 contents and radiogenic isotopes

OIB melting regimes are primarily shaped by lithospheric thickness. Fig. 8a is a schematic cartoon based on experimental studies (see compilation of Hirschmann and

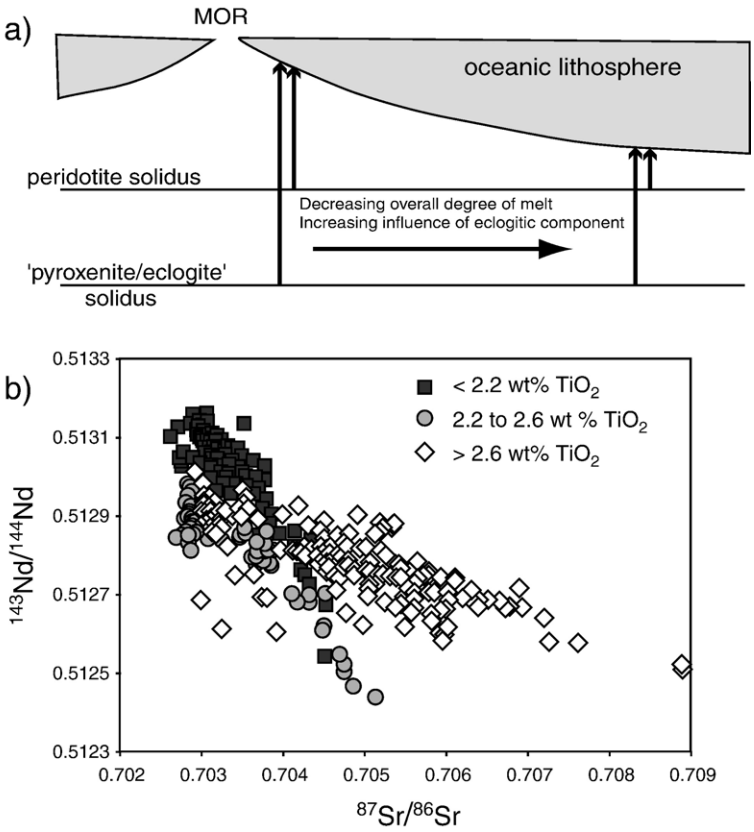

Fig. 8. a) Schematic cartoon illustrating the effect of increasing lithospheric thickness on the manifestation of an eclogitic signature in erupted melts. b) Sr–Nd isotopic compositions of OIB from the GEOROC database. Only samples with major element data used in determining the reference TiO_2 values of OIB are plotted. Samples are shaded in progressively lighter grey scale as their reference TiO_2 content increases.

Stolper, 1996) showing that the onset of eclogite melting occurs at significantly higher pressures than for peridotites. Thick lithosphere restricts the amount of peridotite melting and therefore limits the dilution of eclogitic melts. Therefore, in OIB settings the eclogitic signature should be more apparent in lower degree melts under thicker lithosphere rather than higher degree melts under thinner lithosphere. Fig. 8b shows isotopic analyses from the same samples used in our compilation of OIB major element data shaded by reference TiO_2 abundance. The darker colors, indicating less Ti and larger degrees of melt, plot in fairly restricted Sr–Nd isotopic ranges (e.g. Iceland, Hawaii). OIB localities with larger compositional variation in Sr–Nd space have lower inferred degrees of melt and higher TiO_2 content. Therefore, smaller degree melts appear to preserve more extreme isotopic signatures than larger degree melts (e.g., Phipps Morgan and Morgan, 1999; Regelous et al., 2003; Sims and Hart, 2006). It thus follows that smaller degree melts may contain a larger proportion of the more readily fusible component, which carries the enriched isotopic signatures. The inferred smaller degree melts have a wide range of isotopic values from depleted to very enriched (e.g São Miguel, Society Islands). Therefore, they may be able to sample spatially distinct parts of their source. Whilst a mixed eclogite-peridotite source would be expected to show such a melting behavior, recycled oceanic crust alone cannot account for the most extreme isotopic signatures. Additional, associated components are required (e.g. Niu and O'Hara, 2003; Stracke et al., 2003 and Fig. 7) that may also be preferentially sampled in a manner similar to the basaltic component discussed above.

The involvement of mafic crust in the OIB source clearly does not preclude the further presence of small amounts of sediment or recycled lithosphere containing metasomatic veins or other components. The latter components are not required by the Ti constraints but appear necessary from radiogenic isotopes. Consequently, there is no need for various means of enrichment to be mutually exclusive. Indeed, they may complement one another, and a recycled component may be readily envisaged as comprising portions of mafic crust (with or

without sediment) and the originally underlying metasomatised oceanic lithosphere. The degree of melt may then form a dominant control on the sampling of enriched signatures derived from such a mixed source.

6. Summary

In a global dataset of OIB compositions, we observe that most TiO_2 contents cannot be generated from any plausible peridotitic sources. This is a robust result, as our estimation of both bulk partition coefficient and primitive 'reference' TiO_2 values are conservatively determined. Sediments and lithosphere metasomatised by small degree melts are found to be either inadequate to reconcile our observations, or would have other geochemical consequences that are not apparent. Small amounts (generally less than 10%) of recycled oceanic crust to peridotitic mantle is an attractive, geochemically consistent explanation for the enrichment of Ti in OIB.

Acknowledgements

JP acknowledges financial support from a postgraduate Overseas Research Scholarship from the British council, a University of Bristol postgraduate scholarship, and a postgraduate NSERC overseas scholarship from the Canadian federal government. We thank M. J. Walter and J. Blundy for many helpful discussions, R. Dasgupta for providing a preprint of his work and M. Hirschmann for further words of wisdom. We are grateful for two anonymous reviews that helped us clarify our arguments. We appreciate the comments of M. Willbold, S. Kohn, and M.J. Walter on a version of the manuscript and are also indebted to K. Klimm, R. Avanzinelli, D. Schmidt and Q. House for stimulating conversations.

Appendix A. Supplementary data

Supplementary data associated with this article can be found, in the online version, at doi:10.1016/j.epsl.2007.09.015.

References

Albarède, F., Tamagnan, V., 1988. Modeling the recent geochemical evolution of the Piton de la Fournaise volcano, Reunion Island. 1931–1986. J. Pet. 29, 997–1030.

Becker, H., Jochum, K.P., Carlson, R.W., 2000. Trace element fractionation during dehydration of eclogites from high pressure terranes and the implications for elemental fluxes in subduction zones. Chem. Geol. 163, 65–99.

Beyer, E.E., Griffin, W.L., O'Reilly, S.Y., 2006. Transformation of Archean Lithospheric Mantle by refertilization: evidence from exposed peridotites in the western gneiss region, Norway. J. Pet. 47, 1611–1636.

Boyet, M., Carlson, R.W., 2005. ^{142}Nd evidence for early (>4.53 Ga) global differentiation of the silicate earth. Science 309, 576–581.

Bryan, W.B., Dick, H.J.B., 1982. Contrasted abyssal basalt liquidus trends: evidence for mantle major element heterogeneity. Earth Planet. Sci. Lett. 58, 15–26.

Blundy, J.D., Falloon, T.J., Wood, B.J., Dalton, J.A., 1995. Sodium partitioning between clinopyroxene and silicate melts. J. Geophys. Res. 100, 15501–15515.

Cannat, M., Briais, A., Deplus, C., Escartin, J., Georgen, J., Lin, J., Mercouriev, S., Meyzen, C., Muller, M., Pouliquen, G., et al., 1999. Mid-Atlantic Ridge-Azores hotspot interactions: along axis migration of a hotspot-derived event of enhanced magmatism 10 to 4 Ma ago. Earth Planet. Sci. Lett. 173, 257–269.

Chase, C.G., 1981. Ocean Island Pb: two-stage histories and mantle evolution. Earth Planet. Sci. Lett. 52, 277–284.

Dasgupta, R., Hirschmann, M.M., Stalker, K., 2006. Immiscible transition from carbonate-rich to silicate-rich melts in the 3 GPa melting interval of eclogite+CO_2 and the genesis of silica-undersaturated ocean island lavas. J. Pet. 47, 647–671.

Dasgupta, R., Hirschmann, M.M., Smith, N.D., in press. Partial melting experiments of peridotite+CO_2 at 3 GPa and genesis of alkalic ocean island basalts. J. Pet. doi:10.1093/petrology/egm053.

Ellam, R.M., 1992. Lithospheric thickness as a control on basalt geochemistry. Geology 20, 153–156.

Elliott, T., Blichert-Toft, J., Heumann, A., Koetsier, G., Forjaz, V., 2007. The origin of enriched mantle beneath São Miguel, Azores. Geochim. Cosmochim. Acta 71, 219–240.

Fretzdorff, S., Haase, K.M., 2002. Geochemistry and petrology of lavas from the submarine flanks of Reunion Island (western Indian Ocean): implications for magma genesis and the mantle source. Min. Pet. 75, 153–184.

Frey, F.A., Garcia, M.O., Roden, M.F., 1994. Geochemical characteristics of Koolau volcano: Implications of intershield geochemical differences among Hawaiian volcanoes. Geochim. Cosmochim. Acta 58, 1441–1462.

Gast, P.W., Tilton, G.R., Hedge, C., 1964. Isotopic composition of lead and strontium from Ascension and Gough Islands. Science 145, 1181–1185.

Haase, K.M., 1996. The relationship between the age of the lithosphere and the composition of oceanic magmas: constraints on partial melting, mantle source and the thermal structure of plates. Earth Planet. Sci. Lett. 144, 75–92.

Halliday, A.N., Lee, D.-L., Tommasini, S., Davies, G.R., Paslick, C.R., Fitton, J.G., James, D.E., 1995. Incompatible trace elements in OIB and MORB and source enrichment in the sub-oceanic mantle. Earth Planet. Sci. Lett. 133, 379–395.

Hart, S.R., Hauri, E.H., Oschmann, L.A., Whitehead, J.A., 1992. Mantle plumes and entrainment – isotopic evidence. Science 256, 517–520.

Hawkesworth, C.J., Mantovani, M.S.M., Taylor, P.N., Palacz, Z., 1986. Evidence for the Parana of south Brazil for a continental contribution to DUPAL basalts. Nature 322, 356–359.

Hellebrand, E., Snow, J.E., Hoppe, P., Hofmann, A.W., 2002. Garnet-field melting and late-stage refertilization in 'residual' abyssal peridotites from the central Indian ridge. J. Pet. 43, 2305–2338.

Hémond, C., Devey, C.W., Chauvel, C., 1994. Source compositions and melting processes in the Society and Austral plumes (South Pacific Ocean): element and isotope (Sr, Nd, Pb, Th) geochemistry. Chem. Geol. 115, 7–45.

Hill, E., 2000. PhD. thesis, University of Bristol.

Hill, E., Wood, B.J., Blundy, J.D., 2000. The effect of Ca-Tschermarks component on trace element partitioning between clinopyroxene and silicate melt. Lithos 53, 205–217.

Hirschmann, M.M., Stolper, E.M., 1996. A possible role for garnet pyroxenite in the origin of the 'garnet signature' in MORB. Contrib. Mineral. Petrol. 124, 185–208.

Hirschmann, M.M., Kogiso, T., Baker, M.B., Stolper, E.M., 2003. Alkalic magmas generated by partial melting of garnet pyroxenite. Geology 31, 481–484.

Hofmann, A.W., White, W.M., 1982. Mantle plumes from ancient oceanic crust. Earth Planet. Sci. Lett. 57, 421–436.

Johnson, K.T.M., Dick, H.J.B., Shimizu, N., 1990. Melting in the oceanic upper mantle; an ion microprobe study of diopsides in abyssal peridotites. J. Geophys. Res. 95, 2661–2678.

Kelley, K.A., Plank, T., Ludden, J., Staudigel, H., 2003. Composition of altered oceanic crust at ODP Sites 801 and 1149. G-Cubed, vol 4 no 6. doi:10.1029/2002GC000435.

Kempton, P.D., 1987. Mineralogical and geochemical evidence for differing styles of metasomatism in spinel lherzolite xenoliths: enriched mantle source regions of basalts. In: Menzies, M.A., Hawkesworth, C.J. (Eds.), Mantle metasomatism. Academic Press Inc, pp. 45–90.

Kinzler, R.J., 1997. Melting of mantle peridotite at pressures approaching the spinel to garnet transition. J. Geophys. Res. 102, 865–874.

Kinzler, R.J., Grove, T.L., 1992. Primary magmas of mid-ocean ridge basalts: 1. Experiments and methods. J. Geophys. Res. 97, 6885–6906.

Klein, E.M., Langmuir, C.H., 1987. Global correlations of ocean ridge basalt chemistry with axial depth and crustal thickness. J. Geophys. Res. 92, 8089–8115.

Kogiso, T., Hirose, K., Takahashi, E., 1998. Melting experiments on homogenous mixtures of peridotite and basalt: application to the genesis of ocean island basalts. Earth Planet. Sci. Lett. 162, 45–61.

Kogiso, T., Hirschmann, M.M., Frost, D.J., 2003. High-pressure partial melting of garnet pyroxenite: possible mafic lithologies in the source of ocean island basalts. Earth Planet. Sci. Lett. 216, 603–617.

Langmuir, C.H., Bender, J.F., Bence, A.E., Hanson, G.N., Taylor, S.R., 1977. Petrogenesis of basalts from the FAMOUS area: mid-Atlantic ridge. Earth Planet. Sci. Lett. 36, 133–156.

Langmuir, C.H., Klein, E.M., Plank, T., 1992. Petrological systematics of mid-ocean ridge basalts: constraints on melt generation beneath ocean ridges. Geophysical Monograph 71 'Mantle Flow and melt generation at Mid-ocean ridges', pp. 183–280.

Litvin, Y.A., Gasparik, T., 1993. Melting of jadeite to 16.5 GPa and melting relationships on the enstatite-jadeite join. Geochim. Cosmochim. Acta 57, 2033–2040.

Longhi, J., 2002. Some phase equilibrium systematics of lherzolite melting: I. Geochem. Geophys. Geosyst. 3. doi:10.1029/2001GC000204.

Lundstrom, C.C., Shaw, H.F., Ryerson, F.J., Williams, Q., Gill, J., 1998. Crystal chemical control of clinopyroxene-melt partitioning in the Di-Ab-An system: Implications for elemental fractionations in the depleted mantle. Geochim. Cosmochim. Acta 62, 2849–2862.

McBirney, A.R., Gass, I.G., 1967. Relations of oceanic volcanic rocks to mid-oceanic rises and heat flow. Earth. Planet. Sci. Lett. 2, 265–276.

McDade, P., Blundy, J.D., Wood, B.J., 2003. Trace element partitioning on the Tinaquillo Lherzolite solidus at 1.5 GPa. Phys. Earth Planet. Inter. 139, 129–147.

McKenzie, D., O'Nions, R.K., 1983. Mantle Reserviors and ocean island basalts. Nature 301, 229–231.

McKenzie, D., Bickle, M.J., 1988. The volume and composition of melt generated by extension of the lithosphere. J. Pet. 29, 625–679.

McKenzie, D., O'Nions, R.K., 1991. Partial melt distributions from inversion of rare earth element concentrations. J. Pet. 32, 1021–1091.

McKenzie, D., O'Nions, R.K., 1995. The source regions of ocean island basalts. J. Pet. 36, 133–159.

McKenzie, D., Stracke, A., Blichert-Toft, J., Albarède, F., Gronvold, K., O'Nions, K., 2004. Source enrichment processes responsible for isotopic anomalies in oceanic island basalts. Geochim. Cosmochim. Acta 68, 2699–2724.

Niu, Y., 1997. Mantle melting and melt extraction processes beneath ocean ridges: Evidence from abyssal peridotites. J. Pet. 38, 1047–1074.

Niu, Y., O'Hara, M.J., 2003. Origin of ocean island basalts: a new perspective from petrology, geochemistry, and mineral physics considerations. J. Geophys. Res. 108, 2209. doi:10.1029/2002JB002048.

Niu, Y., Regelous, M., Wendt, I.J., Batiza, R., O'Hara, M.J., 2002. Geochemistry of near-EPR seamounts: importance of source vs. process and the origin of enriched mantle component. Earth Planet. Sci. Lett. 199, 327–345.

Norman, M.D., Garcia, M.O., 1999. Primitive magmas and source characteristics of the Hawaiian plume: petrology and geochemistry of shield picrites. Earth Planet. Sci. Lett. 168, 27–44.

Parman, S.W., Grove, T.L., 2004. Harzburgite melting with and without H_2O: Experimental data and predictive modeling. J. Geophys. Res. 109, B02201.

Pertermann, M., Hirschmann, M.M., 2003. Anhydrous partial melting experiments on MORB-like eclogite: phase relations, phase compositions and mineral-melt partitioning of major elements at 2-3 GPa. J. Pet. 44, 2173–2201.

Pertermann, M., Hirschmann, M.M., Hametner, K., Günther, D., Schmidt, M.W., 2004. Experimental determination of trace element partitioning between garnet and silica-rich liquid during anhydrous partial melting of MORB-like ecolgite. Geochem. Geophys. Geosyst. 5. doi:10.1029/2003GC000638.

Phipps Morgan, J., Morgan, W.J., 1999. Two-stage melting and the geochemical evolution of the mantle: a recipe for mantle plum-pudding. Earth Planet. Sci. Lett. 170, 215–239.

Pilet, S., Hernandez, J., Slyvester, P., Poujol, M., 2005. The metasomatic alternative for ocean island basalt chemical heterogeneity. Earth Planet. Sci. Lett. 236, 148–166.

Plank, T., Langmuir, C.H., 1998. The chemical composition of subducting sediments and its consequences for the crust and mantle. Chem. Geol. 145, 325–394.

Prytulak, J., Vervoort, J., Plank, T., Yu, C., 2006. Astoria Fan sediments, DSDP site 174, Cascadia Basin: Hf–Nd–Pb constraints on provenance and outburst flooding. Chem. Geol. 233, 276–292.

Regelous, M., Hofmann, A.W., Abouchami, W., Galer, S.J.G., 2003. Geochemistry of lavas from the Emperor Seamounts, and the geochemical evolution of Hawaiian magmatism from 85 to 42 Ma. J. Pet. 44, 113–140.

Ribe, N.M., 1985. The generation and composition of partial melts in the Earths mantle. Earth Planet. Sci. Lett. 73, 361–376.

Richter, F.M., 1986. Simple models for trace element fractionation during melt segregation. Earth Planet. Sci. Lett. 77, 333–344.

Rudnick, R.L., Gao, S., 2004. In: Rudnick, R.L., Holland, H.D., Turekian, K.K. (Eds.), Composition of the Continental Crust. Treatise on Geochemistry, Volume 3, The Crust. Elsevier, pp. 1–64.

Salters, V.J.M., 1996. The generation of mid-ocean ridge basalts from the Hf and Nd isotope perspective. Earth Planet. Sci. Lett. 141, 109–123.

Salters, V.J.M., Longhi, J., 1999. Trace element partitioning during the initial stages of melting beneath mid-ocean ridges. Earth Planet. Sci. Lett. 166, 15–30.

Searle, R.C., 1980. Tectonic patterns of the Azores spreading center and triple junction. Earth Planet. Sci. Lett. 51, 415–434.

Shaw, D.M., 1970. Trace element fractionation during anatexis, Geochim. Cosmochim. Acta 34, 237–243.

Sims, K.W.W., Hart, S.R., 2006. Comparison of Th, Sr, Nd, and Pb isotopes in oceanic basalts: Implications for mantle heterogeneity and magma genesis. Earth Planet. Sci. Lett. 245, 743–761.

Sobolev, A.V., Hofmann, A.W., Sobolev, S.V., Nikogosian, I.K., 2005. An olivine-free mantle source of Hawaiian shield basalts. Nature 434, 590–597.

Sobolev, A.V., Hofmann, A.W., Kuzmin, D.V., Yaxley, G.M., Arndt, N.T., Chung, S.-L., Danyushevsky, L.V., Elliott, T., Frey, F.A., Garcia, M.O., et al., 2007. The amount of recycled crust in sources of mantle-derived melts. Science 316, 412–417.

Stracke, A., Bizimis, M., Salters, V.J.M., 2003. Recycling oceanic crust: quantitative constraints. Geochem. Geophys. Geosyst. 4. doi:10.1029/2001GC000223.

Sun, S.-S., McDonough, W.F., 1989. Chemical and isotopic systematics of oceanic basalts: implications for mantle composition and processes. In: Saunders, A.D., Norry, M.J. (Eds.), Magmatism in the ocean basins. Geol. Soc. Spec. Publ., vol. 42. Blackwell Scientific Publ., London, pp. 313–346.

van Westrenen, W., Blundy, J., Wood, B., 1999. Crystal-chemical controls on trace element partitioning between garnet and anhydrous silicate melt. Am. Mineral. 84, 838–847.

Vervoort, J.D., Patchett, P.J., Blichert-Toft, J., Albarède, F., 1999. Relationship between Lu–Hf and Sm–Nd isotopic systems in the global sedimentary system. Earth Planet. Sci. Lett. 168, 79–99.

Walter, M.J., 1998. Melting of garnet peridotite and the origin of komatiite and depleted lithosphere. J. Pet. 39, 29–60.

Watson, S., McKenzie, D., 1991. Melt generation by plumes: a study of Hawaiian volcanism. J. Pet. 32, 501–537.

Weaver, B.L., 1991. The origin of ocean island basalt endmember compositions: trace element and isotopic constraints. Earth Planet Sci. Lett. 104, 381–397.

Wood, B.J., Blundy, J., 2003. Trace element partitioning under crustal and uppermost mantle conditions: the influence of ionic radius, cation charge, pressure, and temperature. Treatise Geochem. 2, 395–423.

Workman, R.K., Hart, S.R., 2005. Major and trace element composition of the depleted MORB mantle (DMM). Earth Planet. Sci. Lett. 231, 53–72.

Workman, R.K., Hart, S.R., Jackson, M., Regelous, M., Farley, K.A., Blusztajn, J., Kurz, M., Staudigel, H., 2004. Recycled metasomatized lithosphere as the origin of the Enriched Mantle II (EM2) endmember: evidence from the Samoan volcanic chain. Geochem. Geophys. Geosyst. 5. doi:10.1029/2003GC000623.

Zindler, A., Hart, S., 1986. Chemical geodynamics. Ann. Rev. Earth Planet. Sci. 14, 493–571.